ACS OMEGA

http://pubs.acs.org/journal/acsodf

Article

Detection of Glutamate Encapsulated in Liposomes by Optical Trapping Raman Spectroscopy

Kyoko Masui, Yasunori Nawa, Shunsuke Tokumitsu, Takahiro Nagano, Makoto Kawarai, Hirokazu Tanaka, Tatsuki Hamamoto, Wataru Minoshima, Tomomi Tani, Satoshi Fujita, Hidekazu Ishitobi, Chie Hosokawa,* and Yasushi Inouye*

Cite This: *ACS Omega* 2022, 7, 9701−9709

Read Online

ACCESS | Metrics & More | Article Recommendations

ABSTRACT: The transmission of neuronal information is propagated through synapses by neurotransmitters released from presynapses to postsynapses. Neurotransmitters released from the presynaptic vesicles activate receptors on the postsynaptic membrane. Glutamate acts as a major excitatory neurotransmitter for synaptic vesicles in the central nervous system. Determining the concentration of glutamate in single synaptic vesicles is essential for understanding the mechanisms of neuronal activation by glutamate in normal brain functions as well as in neurological diseases. However, it is difficult to detect and quantitatively measure the concentration of glutamate in single synaptic vesicles owing to their small size, i.e., ∼40 nm. In this study, to quantitatively evaluate the concentrations of the contents in small membrane-bound vesicles, we developed an optical trapping Raman spectroscopic system that analyzes the Raman spectra of small objects captured using optical trapping. Using artificial liposomes encapsulating glutamate that mimic synaptic vesicles, we investigated whether spontaneous Raman scattered light of glutamate can be detected from vesicles trapped at the focus using optical forces. A 575 nm laser beam was used to simultaneously perform the optical trapping of liposomes and the detection of the spontaneous Raman scattered light. The intensity of Raman scattered light that corresponds to lipid bilayers increased with time. This observation suggested that the number of liposomes increased at the focal point. The number of glutamate molecules in the trapped liposomes was estimated from the calibration curve of the Raman spectra of glutamate solutions with known concentration. This method can be used to measure the number of glutamate molecules encapsulated in synaptic vesicles *in situ*.

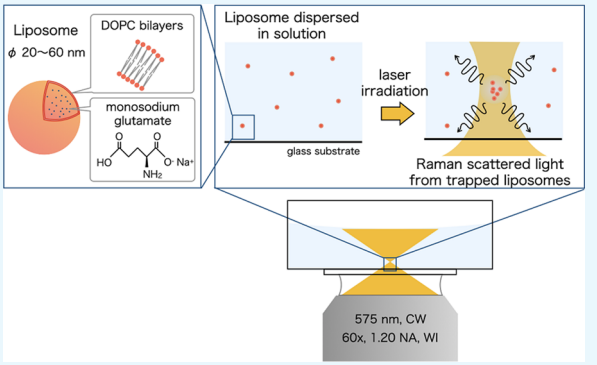

1. INTRODUCTION

Neurotransmitters that are stored in the synaptic vesicles of the presynaptic terminals of neurons play a central role in transmitting neuronal information through synapses. Among these, glutamate is a major excitatory neurotransmitter used in the central nervous system.[1−4] The number of glutamate molecules in synaptic vesicles had been previously estimated using a radioreceptor assay,[5] immunoisolation,[6] and the enzyme-based amperometric method,[7] assuming their concentration in a single vesicle to be around 50−100 mM or even higher. However, it remains a challenge to quantitatively measure the concentration of *in situ* glutamate molecules in living neuronal cells, owing to the small size (∼40 nm in diameter) of the vesicles.[8−10]

Spontaneous Raman spectroscopy is a label-free quantitative analysis method that allows a nondestructive and direct analysis of molecular structures and concentrations. The shift in the wavelength of the incident light undergoing Raman scattering depends on the interaction between the incident light and the molecule, thus, enabling an accurate detection of the concerned molecule. Additionally, the intensity of the Raman scattered light is linearly proportional to the number of molecules. Therefore, the use of Raman spectroscopy allows us to analyze molecular species and quantitatively monitor the concentrations of molecules in samples under *in vivo* and *in vitro* conditions.[11,12] By combining Raman spectroscopy with optical trapping techniques, it has been reported that glutamate released from a single synaptosome can be detected *in situ* without any damage.[13,14] Synaptosomes are components isolated from the synaptic terminals, which maintain some of the synaptic activities such as the uptake, storage, and release

Received: December 21, 2021
Accepted: February 10, 2022
Published: February 28, 2022

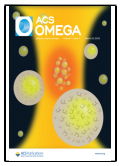

https://doi.org/10.1021/acsomega.1c07206
ACS Omega 2022, 7, 9701−9709

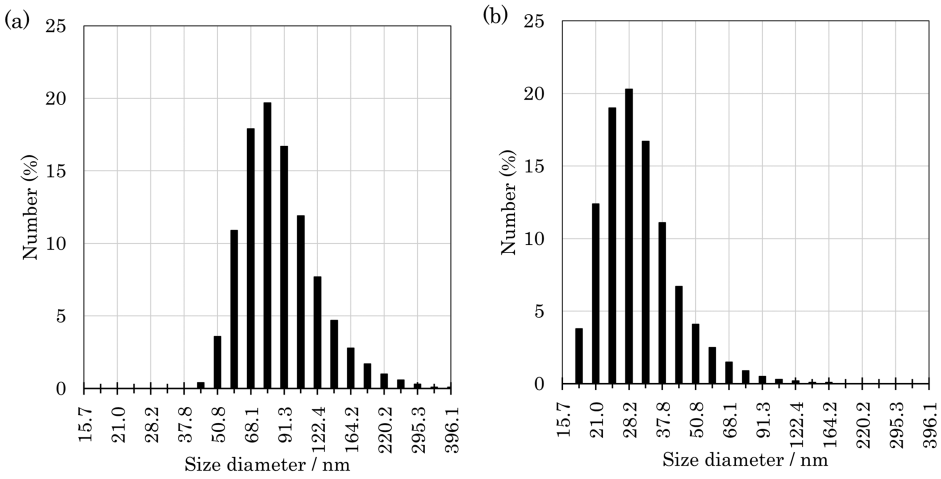

Figure 1. Size of the synthesized liposomes measured using DLS. (a) Synthesized liposomes filtered through 800 and 100 nm polycarbonate filters and (b) liposomes sonicated for 3 h after step (a).

of neurotransmitters even after isolation. The synaptosome from a rat brain is ∼600 nm in diameter and contains multiple synaptic vesicles. Glutamate molecules were released from optically trapped synaptosomes during exocytosis in the presence of the potassium channel blocker 4-aminopyridine that triggers repetitive firing of voltage-gated sodium channels in synaptosomes. The estimated amount of glutamate released from a single synaptosome was measured to be ∼3 attomole.[13,14] In spite of successful detection of glutamate molecules from isolated synaptosomes and vesicles dispersed in a solution, it has been challenging to measure the number of glutamate molecules stored in single synapses of living neuronal cells due to the size of synaptic vesicles and the small volume of the synaptic region. One of the solutions is to use Raman spectroscopy on multiple synaptic vesicles gathered in the focal volume with the aid of optical trapping.

Optical tweezers, which manipulate micro/nanoparticles using the optical gradient force generated by a laser beam focused tightly under an objective lens, are used as optical trapping techniques. It has been reported that optical trapping can concentrate synaptic vesicles at the focal point in living neuronal cells.[21] Raman spectroscopy can enable the quantitative analysis of any molecule. Therefore, combined with optical trapping, Raman scattered light can be obtained from trapped objects.[13−20,22−24] This method would be useful to identify glutamate molecules encapsulated in synaptic vesicles. In this study, we demonstrated the detection of Raman scattered lights from optically trapped nanosize artificial liposomes encapsulating glutamate solutions. We prepared artificial liposomes that mimic synaptic vesicles for detecting spontaneous Raman scattered light of glutamate molecules from multiple vesicles trapped at the focal point. We have also discussed the application of optical trapping Raman spectroscopy based on our experimental data and estimated the number of glutamate molecules encapsulated in nanoscale liposomes that mimic synaptic vesicles.

2. RESULTS AND DISCUSSION

2.1. Liposomal Formation. Artificial liposomes[25,26] that mimic synaptic vesicles were prepared using 1,2-dioleoyl-*sn*-glycero-3-phosphocholine (DOPC), which is one of the components of synaptic vesicles.[8] Liposomes were prepared by adding glutamate solutions with various concentrations to lipid membranes dried in a glass vial, passed through two different filters with different pore sizes and ultrasonicated to reduce the size. The external solution was replaced with a buffer solution without glutamate using gel chromatography. The size of liposomes before filtration and sonication was more than 1 μm in diameter, and they were not uniform in shape. After filtration and sonication, the diameter of synthesized liposomes was estimated using dynamic light scattering (DLS) as shown in Figure 1. After extrusion through 800 and 100 nm pore filters, the median size distribution was 78.8 nm (Figure 1a). After 3 h of sonication, the median size of the liposomes changed to 28.2 nm (Figure 1b). The size and shape of the liposomes did not change during the process of gel chromatography. The synthesized liposomes were assumed to be unilamellar lipid bilayers with a thickness of 4.6 nm.[27]

2.2. Peaks of Solutions and Suspensions in Raman Spectra. Raman measurements were performed on solutions at each stage of liposome preparation. The obtained specific peaks were assigned to the vibrational mode according to the references and shown in Table 1. Raman scattered lights from the liposomes were observed when the liposomes were trapped at the focal point. Figure 2 shows the spontaneous Raman spectra of 10 mM 4-(2-hydroxyethyl)-1-piperazineethanesulfonic acid (HEPES) buffer, 500 mM glutamate in 10 mM HEPES buffer, trapped DOPC liposomes with 500 mM NaCl in 10 mM HEPES buffer, and trapped DOPC liposome with

Table 1. Peak Assignment of Raman Spectra

molecule	vibrational mode	wavenumber/cm^{-1}	reference
HEPES	SO_3^- symmetric stretch	1050 (broad)	28
glutamate	C−C−N symmetric stretch	938	13, 14, 29, 30
	CH_2 deformation	1351	
	mixture of the COO^- symmetrical stretching, CH_2 deformation, and symmetrical NH_3^+ deformation	1414	
DOPC	CN symmetric stretching	722	13−15, 17−19, 31
	C−C skeletal stretching	1080	
	CH_2 bend scissoring	1445	
	cis C=C stretching	1650	
	symmetric CH_2 stretching	2850	
	antisymmetric CH_2 stretching	2880	

https://doi.org/10.1021/acsomega.1c07206
ACS Omega 2022, 7, 9701−9709

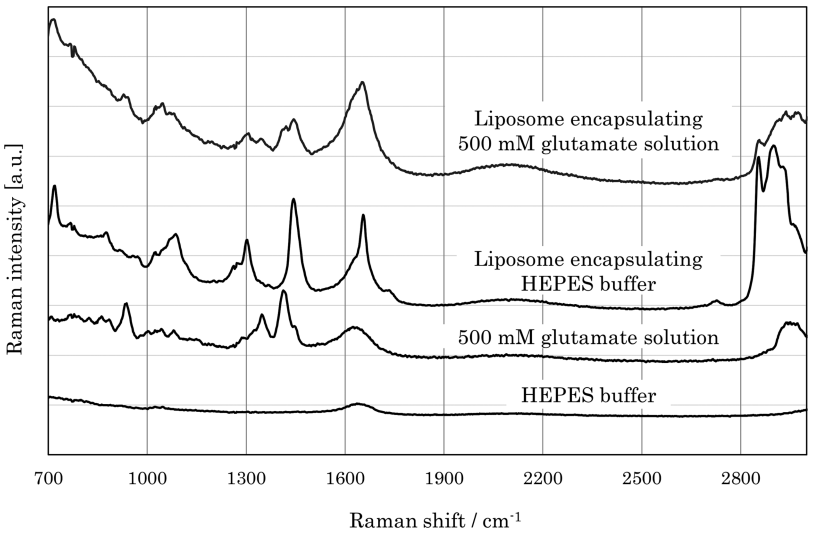

Figure 2. From top: Raman spectra of trapped DOPC liposomes encapsulating 500 mM glutamate in 10 mM HEPES buffer, trapped DOPC liposomes encapsulating 500 mM NaCl in 10 mM HEPES buffer, 10 mM HEPES buffer with 500 mM glutamate, and 10 mM HEPES buffer.

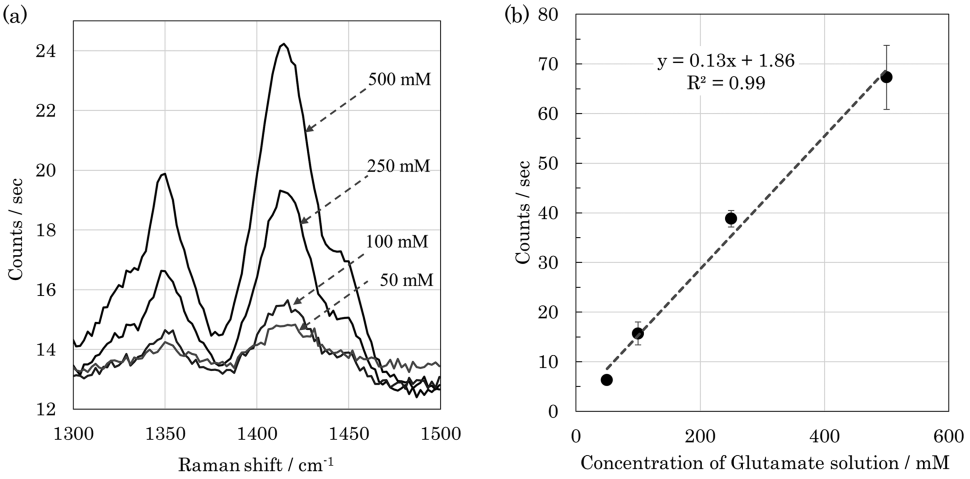

Figure 3. (a) From top to bottom: Raman spectra of 500, 250, 100, and 50 mM of glutamate solution. (b) Calibration curve of Raman intensity counts versus concentration of glutamate solutions in the range of 1383−1429 cm^{-1} of each spectrum (N = 3).

500 mM glutamate in 10 mM HEPES buffer, respectively. The Raman spectra shown in Figure 2 are averaged values of 600 spectra acquired with 1 s exposure using a 575 nm laser wavelength and 3.9 mW laser power. Broad background signals of the glass substrate and water were observed in all of the spectra.

Although the SO_3^- symmetric stretching mode was obtained in the original HEPES solution, it was buried by the specific peaks of other molecules dispersed in the HEPES solution and was not detected in other spectra. In the spectrum of glutamate solution, the peaks around 1414 cm^{-1} are a mixture of the COO^- symmetrical stretching mode, CH_2 deformation mode, and the symmetrical NH_3^+ deformation mode in which the peak values are difficult to separate because of the wavenumber resolution. The salient peaks of DOPC were obtained from both the liposome suspensions. In our study, we used Raman peaks at 1414 and 2850 cm^{-1} to identify the presence of glutamate molecules and lipid, respectively. Some types of amino acids have peaks that shift depending on the ambient environment.[41] Although the ambient environment of glutamate changed upon encapsulation in liposomes, there was no significant peak shift in the Raman spectrum of liposomes encapsulating 500 mM glutamate solution in our experiment.

2.3. Determining the Concentration of Glutamate Molecules Using Raman Spectroscopy. We made a calibration curve of glutamate solutions with a known concentration to determine the number of glutamate molecules from the obtained Raman spectra. Raman measurements were performed for solutions with 50, 100, 250, and 500 mM of glutamate in 10 mM HEPES buffer. The Raman spectra shown in Figure 3 are obtained using a 575 nm laser wavelength and 3.9 mW laser power. Figure 3a depicts the spectra in the range of 1300−1500 cm^{-1}. In this study, the ratiometric analysis method,[42,43] such as using Raman scattering intensities of the wavenumber region of water molecules and lipid molecules, was not utilized since there was concern about the presence of multiple molecules having O−H and C−H groups in the sample solution. The number of counts is defined as the integral value of the polygon enclosed by a straight line connecting the minimum values at both ends of the peak top. To exclude the influence of the lipid-derived peak at 1450 cm^{-1} next to the glutamate-derived peak at 1414 cm^{-1}, the integral value between 1383 and 1429 cm^{-1} was

https://doi.org/10.1021/acsomega.1c07206
ACS Omega 2022, 7, 9701−9709

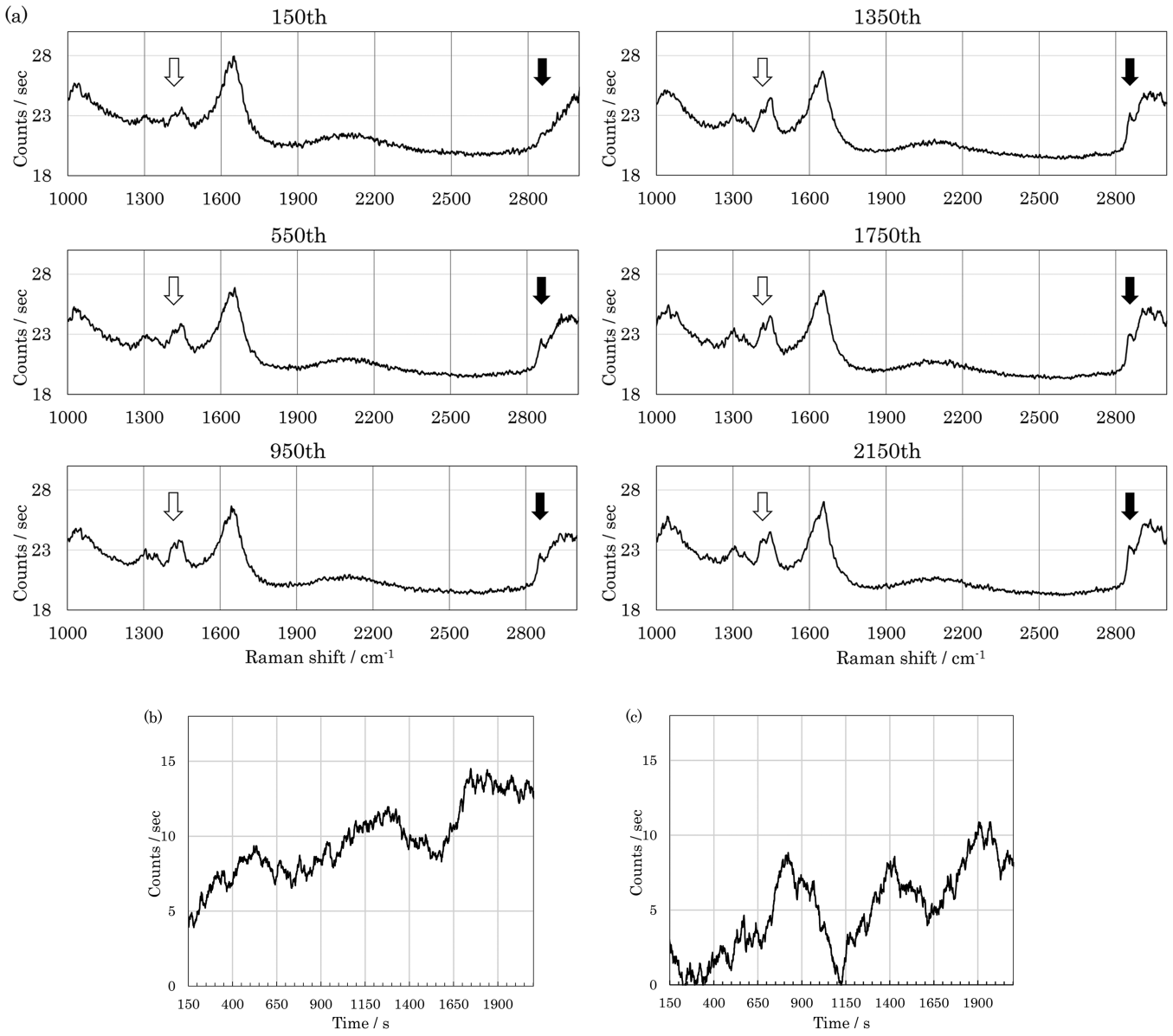

Figure 4. (a) Averaged spectrum of arbitrary multiple time points. Black and white arrows marked at 2850 and 1414 cm^{-1} derived from lipid and glutamate molecules, respectively. Time trace at each peak of (b) 2850 and (c) 1414 cm^{-1}.

obtained as the glutamate-derived counts. The counts detected from glutamate solutions with different concentrations were plotted as shown in Figure 3b. Each averaged spectrum from 1000 measurements with an exposure time of 1 s was obtained for each solution. In Figure 3b, the values are averages of the integral value of the polygon for 1000 spectra, and error bars. The detection limit was calculated to be 21 mM according to the value of dispersion calculated from the mean value of 500 mM and the spectral fluctuations. We confirmed the quantitative relationship between the counts and the concentration of the glutamate solution based on the linearity of the plots. Since Raman intensity depends on the accuracy of the optical setup and/or sample preparation, calibration curves for each experiment are required for every measurement.

To estimate the number of glutamate molecules in the focal volume, the volume of the laser spot of a linearly polarized laser of 575 nm was calculated with an objective lens of 1.20 numerical aperture of objective lens. The Gaussian integral of focal volume was calculated to be 5.7×10^7 nm^3. A total of $\sim 1.7 \times 10^7$ of glutamate molecules exist in the 500 mM glutamate solution. The horizontal axis of the calibration curve can be converted to the number of glutamate molecules.

2.4. Time Tracing of Raman Counts from Optically Trapped Liposomes. The temporal dynamics of the trapped liposomes was examined by continuously irradiating the liposome suspension with a laser. Raman spectra of the optically trapped liposomes encapsulating the 500 mM glutamate solution were acquired 2400 times consecutively with a 1 s exposure interval. To reduce the fluctuations of each spectrum, the average spectrum of 149 spectra before and after each time point was obtained as moving averages for 299 spectra. In the case of the 150th spectrum, the count at each wavenumber shows the average count between 1 and 299 s. The resulting spectra of arbitrary multiple time points are shown in Figure 4a. Raman peaks at 2850 and 1414 cm^{-1}, indicating the existence of liposomes and glutamate molecules, appeared in all spectra. The count value was defined as a signal when the difference between the peak top and bottom was

https://doi.org/10.1021/acsomega.1c07206
ACS Omega 2022, 7, 9701−9709

more than three times the standard deviation of the counts at the bottom. To investigate the behavior of the count change in detail, the time variation of counts per second were examined for each 2850 and 1414 cm^{-1} peak. For the 2400 original data, the integral values from 2834 to 2868 cm^{-1} and from 1383 to 1429 cm^{-1} were plotted as lipid-derived counts and glutamate-derived counts, respectively. Typical examples of time traces from 150 to 2251 s out of a total of 2400 original data are shown in Figure 4b,c.

The counts of the 2850 cm^{-1} peak derived from the lipid increased with time, as shown in Figure 4b. This implies that the liposomes were trapped around the focal point by the optical forces and the trapped number gradually increased with respect to the irradiation time. The count at each point changed because the size and/or the number of trapped liposomes at each point were not the same. This observation was consistent with the DLS result that showed variations in the size and number of liposomes in the prepared solution. It should be noted that the Raman scattered light could be detected from liposomes that transiently passed through the focal point. The number of liposomes cannot be estimated from the result of Figure 4b because it is difficult to estimate the intensity of Raman scattered light per liposome due to the current detection limit.

By considering the probability of liposomes trapped by the optical forces at the focal point, we estimated the number of trapped liposomes under our experimental conditions. The optical trapping potential energy U is defined as $U = -\alpha|E|^2/2$, where α is the polarizability of a single liposome and E is the electric field of the focused laser beam. Furthermore, α is defined as $\alpha = \frac{4\pi\varepsilon_2 a^3[(n_1/n_2)^2 - 1]}{[(n_1/n_2)^2 + 2]}$, where ε_2 is the dielectric constant of the surrounding medium, a is the radius of the liposome, and n_1 and n_2 are the refractive indices of the liposome and the medium, respectively. For a stable trapping of a liposome in the medium, the optical trapping potential energy $|U|$ should exceed the thermal energy 10 kT,[15] where k is the Boltzmann constant and T is the temperature. Under our experimental conditions, the refractive index of the encapsulating solution and the outer solution was measured by our attenuated total reflection spectroscopy to be 1.334 and that of the DOPC bilayer was set at 1.456.[32] Considering that the thickness of the DOPC bilayer was 4.6 nm[27] and the medial diameter of liposomes was 28.2 nm, from the DLS data, the refractive index of a single liposome was calculated to be 1.419. The three-dimensional diameter of the focal point was calculated from the light intensity distribution obtained by numerical calculations using the imaging theory and then the volume of the focal point was calculated. Since the effective diameter in the transverse direction shows a strong dependence on the polarization of the irradiation light,[33] the beam waist of the laser focus, which is an elapse focus shape in the $X-Y$ plane, was assumed to be 188 and 254 nm along the short and long axis, respectively. At a laser power of 3.9 mW, the potential energy $|U|$ to trap a single liposome was estimated to be 0.02 kT, which is indicative of the difficulty to trap a single liposome in the solution in this experimental condition. However, as large number of liposomes were dispersed in the prepared solution, a population of liposomes, which entered the focal point, could be trapped and formed clusters because of the higher trapping potential energy of the cluster than that of a single liposome owing to its relatively higher polarizability and larger size.[21,34,35] Therefore, the formation of the clusters by optical trapping is facilitated under this condition. The estimated results indicate that the clusters formed from more than 500 liposomes can be effectively trapped since the optical trapping potential energy $|U|$ exceeds the thermal energy of 10 kT.

The Raman intensity at 1414 cm^{-1} derived from the glutamate molecule also fluctuated with time as shown in Figure 4c. Time-dependent change of Raman counts from the lipid was different from that from glutamate. This observation was mysterious if lipid and glutamate behave as a single unit (as a liposome) since the counts of Raman scattered light correlate linearly with the number of molecules. If the number of glutamate molecules encapsulated in liposomes was different in different liposomes, this might be the reason for the independent changes of the value for lipid and that for glutamate molecules. It is worth noting that the concentrations of the molecule encapsulated in single liposomes are not consistent when the liposomes are synthesized by the same method that we used.[36] DLS results as shown in Figure 1b depict the variation in the size of the prepared liposomes. The ratio of lipids and encapsulated glutamate molecules is different based on the size difference. Furthermore, there is a possibility that the incoming liposomes rupture at the focal point because of the contentious laser irradiation and optical forces and the encapsulated glutamate molecules diffuse out from the collapsed liposomes. These possibilities might account for the inconsistent time-dependent changes of values for lipid and glutamate in the measurements.

By comparing the results of the calibration curve for glutamate solutions of a known concentration obtained before or after the experiment as explained in Figure 3b, the number of counts can be converted to the number of glutamate molecules. From the calibration curve in Figure 3b, the count of 500 mM glutamate solution acquired with an exposure time of 1 s was 67.3 under the conditions of the experiment shown in Figure 4. At this concentration, 1.7×10^7 of glutamate molecules are present in the focal volume of 5.7×10^7 nm^3. Therefore, the counts from a single glutamate molecule were calculated as 3.9×10^{-6}. The highest count at 1414 cm^{-1} in Figure 4c was 12.5. As a result, this number of counts converted to the number of glutamate molecules was 3.2×10^6. Assuming that all of the trapped liposomes are uniform with 28.2 nm in diameter and the lipid membrane with a thickness of 4.6 nm, the internal volume is 3.6×10^3 nm^3. If 500 mM of glutamate solution is encapsulated in all of the liposomes, the number of glutamate molecules is calculated to be 1.1×10^3. Therefore, the highest count at 1414 cm^{-1} is converted to 3.0×10^3 in the number of liposomes. Since the overall volume of a single liposome with a diameter of 28.2 nm is 1.2×10^4 nm^3, 3.1×10^3 of liposomes can be randomly packed at the focal point for maximum density (64% of the focal volume). In practical terms, the trends in Figure 4b,c were not consistent, and the number of liposomes cannot be estimated from the number of glutamate molecules. As shown in Figure 1b, the size of liposomes varies and it is possible that multiple liposomes form clusters in the prepared solutions. Therefore, it is not feasible to estimate the number of liposomes from the number of glutamate molecules. It is necessary to take the size variation and polydispersity into account to understand the behavior of a single liposome from the results of time trace.

Based on these results, our experiment shows that optical trapping Raman spectroscopy allows us to measure the number

https://doi.org/10.1021/acsomega.1c07206
ACS Omega 2022, 7, 9701−9709

of glutamate molecules encapsulated in the liposomes. With the passage of time, it was confirmed from the intensity distribution of the lipids that the liposomes clustered at a focal point. The fact that the Raman intensity change from glutamate molecules was different from that from lipid was attributed to leakage associated with liposome rupture and fusion caused by prolonged laser irradiation. The surface charge of liposomes composed of DOPC is small and the repulsive force between liposomes is also small. In addition, liposomes exist in high ionic concentrations and have a short Debye length, which increases the chance of contact. As the number of liposomes present in the focal point increases, the possibility of membrane fusion is expected to increase. In the current optical system, the intensity and exposure time of the laser for efficient detection of Raman scattered light and the laser for efficient trapping of liposomes cannot be adjusted separately.

In the present experimental condition, liposomes are dispersed in a solution and are always moving with Brownian motion. Since there was no limit to the space available for diffusion, a long period of laser irradiation was needed to gather the liposomes from distant locations into a focal point. Previous studies have shown that more than 200 vesicles with approximately 1−2 μm diameter are regularly pooled in a confined space in the presynaptic terminal of cultured hippocampal neurons.[21,37,38] Therefore, the time required to trap multiple synaptic vesicles will be reduced. The concentration of glutamate encapsulated in a single synaptic vesicle (40 nm in diameter) is thought to be around 100 mM,[5−7] which means the number of molecules existing in 200 vesicles is 1.8×10^5. Applying this number to the current measurement conditions, the Raman count corresponds to 7.2×10^{-1}. In the current situation, Raman scatted light from synaptic vesicles is difficult to measure due to weak detection sensitivity. However, this can be overcome by optimizing the exposure time and laser intensity. As a way to trap synaptic vesicles without collapsing them, it is also effective to use two different wavelengths of lasers, one for trapping and the other for Raman excitation. If near-infrared light, which is less absorbed by biological molecules, is used as the trapping laser and short wavelength light with a large scattering cross section is used as the excitation laser, then, Raman scattered light can be efficiently detected from the trapped object in a short time. By performing optical trapping Raman spectroscopic measurements at prespecified synaptic sites, it should be possible to efficiently perform quantitative evaluation of glutamate molecules under short exposure conditions. When this optical trapping Raman spectroscopic technique is used for the detection of other molecules, the resonant Raman effect is effective to increase the detection sensitivity. Using an excitation wavelength that is close to or matches the absorption band of the molecule, the intensity of Raman scattered light is expected to be enhanced. Another method is to disperse some metal nanoparticles in a suspension to enhance the intensity by the localized surface plasmon resonance effect. By increasing the intensity of the Raman scattered light that can be obtained at one time, it is expected to be possible to detect and understand the behavior of molecules encapsulated in liposomes, or state changes such as fusion or rupture of liposomes within the focal point.

3. CONCLUSIONS

We performed the optical trapping Raman spectroscopy of liposomes encapsulating glutamate molecules. Scattered light from glutamate molecules and lipid was detected in Raman spectra, indicating that the synthesized liposomes with a median size of 28.2 nm and encapsulated 500 mM glutamate molecules were optically trapped and assembled in the focal point. The time trace of the lipid-derived peak showed that the trapped number of liposomes increased with time. We also estimated the number of glutamate molecules in single liposomes from the calibration curve of glutamate solutions of known concentration. From the focal volume of the excitation laser, the number of liposomes with an average diameter existing in the focal volume was calculated. Our results show that optical trapping Raman spectroscopy would enable us to analyze the behavior of glutamate molecules in synaptic vesicle levels under *in situ* or *in vivo* conditions with some further improvements in time resolution. This finding will play an important role in the development of techniques to detect the concentration of neurotransmitters in the neural network.

4. METHODS

4.1. Chemicals and Gas. Commercially available chemicals were used without any further chemical purification in this research. 1,2-Dioleoyl-*sn*-glycero-3-phosphocholine (DOPC, COATSOME MC-8181, L-α-phosphatidylcholine, 99%, 302-16881) was purchased from FUJIFILM Wako Pure Chemical Corporation (Osaka, Japan). 4-(2-Hydroxyethyl)-1-piperazineethanesulfonic acid (HEPES, 17514-44), monosodium glutamate (16914-92), 1 mol/L hydrochloric acid (37314-15), 1 mol/L sodium hydroxide solution (37421-05), and sodium chloride (191-01665) were purchased from nacalai tesque inc. (Kyoto, Japan). Argon gas and nitrogen gas were purchased from Awao Sangyo (Osaka, Japan). Double-deionized water was purified from tap water using a Milli-Q water purification system (Milli-Q Advantage) from Merck Millipore (Bedford, MA) with a final resistivity of 18.2 MΩ cm and used in the preparation of the solution.

Figure 5 shows the schematic image of the liposomes used in this study. Owing to the weak background signals in Raman measurements, a 10 mM HEPES buffer solution was used as the medium throughout our experiments. Since glutamic acid is slightly soluble in water and the pH of the saturated solution

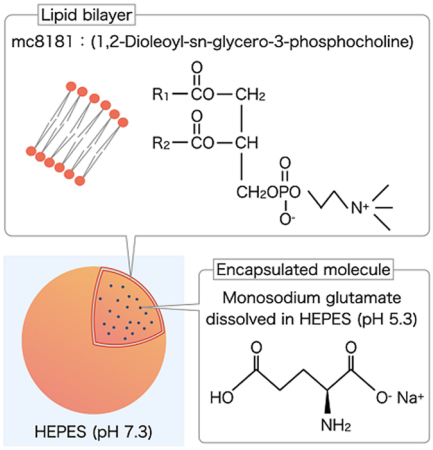

Figure 5. Schematic image of the synthesized liposome.

https://doi.org/10.1021/acsomega.1c07206
ACS Omega 2022, 7, 9701−9709

is about 3.2, 1 M NaOH is used to adjust the pH of 500 mM glutamate solution. The difference between glutamic acid and monosodium glutamate is the terminal part of −OH and −ONa. Since the ionization state and the components of the solution are the same after dissolution at pH 7, monosodium glutamate was also used for this research. In neuronal cells, the pH inside the synaptic vesicles and that of the glutamate ion released to the synaptic cleft are around 5.3 and 7.3, respectively.[39] Therefore, in this study, the pH for the internal solution of liposomes (500 mM glutamate dissolved in 10 mM HEPES buffer) is adjusted to pH 5.3, whereas the pH for the external medium (500 mM NaCl dissolved in 10 mM HEPES buffer) is adjusted to pH 7.3 by adding 1 M HCl and NaOH solutions, respectively.

4.2. Liposome Synthesis. Liposomes formed by a phospholipid bilayer are used as models of membrane-bound vesicles in this study. The liposomes were mainly prepared by following the procedure in ref 40. A stock solution was prepared by dissolving 5 mg of DOPC in 1 mL of chloroform put in a clean light-proof glass vial. The DOPC is one of the main components of the lipid membrane of the synaptic vesicles.[8] This vial was enclosed with argon gas and stored in a −20 °C refrigerator until use. The mixed solution (0.4 mL) was put in a clean 10 mL clear glass vial at room temperature. A thin layer of the mixed solution was made on the wall of the vial by rotating the vial and the evaporation of chloroform was controlled using a stream of nitrogen gas, resulting in the formation of a DOPC film at the wall. The remaining chloroform was removed in a vacuum chamber for at least 6 h. The film was agitated with 2 mL of 500 mM glutamate solution at 45 °C for 1 h, resulting in the formation of liposome suspension encapsulating the 500 mM glutamate solution. For reducing the size of the liposomes, the suspension was extruded using polycarbonate filters with pore diameters of 800 and 100 nm five times each and then sonicated at 43 kHz for 3 h. This procedure is useful to control the size of the liposomes with a unilamellar membrane. Gel filtration columns (illustra NAP-5 Columns, GE Healthcare) were used for exchanging the external solution from 500 mM glutamate solution to 500 mM NaCl HEPES solution. To replace the external solution, 2 mL of the liposome suspension was poured into the column. Each 0.15 mL fraction of the eluted solution was measured using Raman spectroscopy to determine the available volume. The eluate of 0.1 mL in which no glutamate-derived peak was detected in the Raman spectrum was used for the experiment. The size distribution of liposomes was measured using the DLS technique (Zetasizer NanoZS, Malvern Panalytical).

4.3. Optical Setup. Figure 6 shows the schematic diagram of the optical trapping Raman microscope that we have developed. A continuous-wave laser (Genesis MX SLM, Coherent) whose emission wavelength is 575 nm was used as a light source for optical trapping and Raman spectroscopy. The laser light was expanded to a size larger than the pupil size of the objective lens and introduced to the objective lens using a dichroic mirror set in an inverted microscope (Eclipse Ti, Nikon). The suspension of the liposomes encapsulating glutamate in the HEPES buffer was placed on the glass-bottom 12 mm dish (D11130H, Matsunami Glass Ind., Ltd). For optical trapping and Raman measurements, the laser light was focused at 10 μm above the upper surface of the glass dishes using ×60, numerical aperture of 1.20, and a water-immersion objective lens (Plan Apo VC, Nikon). The laser

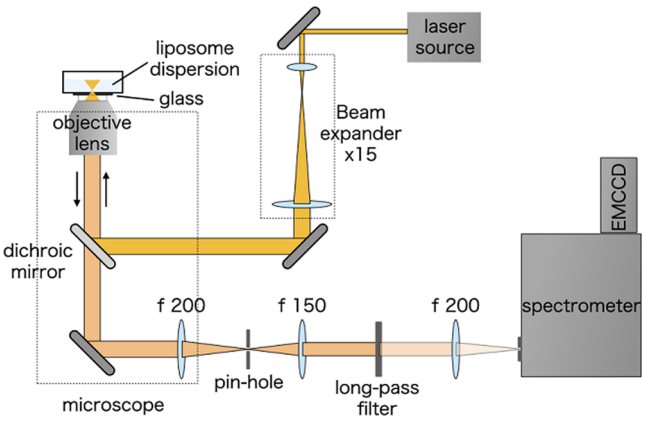

Figure 6. Optical setup of the optical trapping Raman spectroscopy.

power was set as 3.9 mW, as shown in Figures 2−4 at the sample position.

The tightly focused laser light enables trapping of liposomes dispersed in the HEPES buffer, and the backscattered Raman lights from the trapped liposomes were collected by the same objective lens. A pin hole with a 75 μm diameter was set to reduce the scattering from nontrapped particles and stray light. Raman scattered light and Rayleigh scattered light were separated using the long-pass filter (Semrock Brightline 597/LP, OPTO-LINE, Inc.) and subsequently focused to the entrance of the spectrometer (SR-303i-B-N1, Shamrock, Andor Technology). The slit width was set at 100 μm. The filtered Raman scattered light was then dispersed by a grating and captured by a cooled EM-CCD (Newton DU970P-BVFN, Andor, Oxford Instruments). Although the background signals from the out-of-focus region were cut by the pin hole, all of the Raman spectra encapsulate a considerable intensity of signals from water, solvent, and the substrate. The exposure time and EM-CCD gain were set at 1 s and 255 per measurement. To understand the optical trapping dynamics of liposomes using the data of the Raman spectra, the laser light was continuously irradiated, and the Raman spectra were obtained 2400 times.

4.4. Data Treatment. The obtained Raman spectra were analyzed using MATLAB (The MathWorks, Natick). The analysis range of the Raman shift was within 700−3000 cm^{-1}. To perform the analysis, we first picked up a region in a single EM-CCD image, where Raman signals were detected. Then, the offset bias of the EM-CCD detector was subtracted from the selected region and Raman spectra were summed up. In this experiment, 10 Raman spectra were summed up for the analysis. Subsequently, a moving average of 3 pixels in the wavenumber direction was applied.

AUTHOR INFORMATION

Corresponding Authors

Chie Hosokawa − *Advanced Photonics and Biosensing Open Innovation Laboratory, National Institute of Advanced Industrial Science and Technology, Osaka 5650871, Japan; Department of Chemistry, Division of Molecular Materials Science, Graduate School of Science, Osaka City University, Osaka 5588585, Japan;* orcid.org/0000-0002-0289-4680; Email: hosokawa@sci.osaka-cu.ac.jp

Yasushi Inouye − *Advanced Photonics and Biosensing Open Innovation Laboratory, National Institute of Advanced Industrial Science and Technology, Osaka 5650871, Japan; Graduate School of Frontier Biosciences, Osaka University,*

https://doi.org/10.1021/acsomega.1c07206
ACS Omega 2022, 7, 9701−9709

Osaka 5650871, Japan; Department of Applied Physics, Graduate School of Engineering, Osaka University, Osaka 5650871, Japan; orcid.org/0000-0001-5118-5146; Email: ya-inoue@ap.eng.osaka-u.ac.jp

Authors

Kyoko Masui − *Advanced Photonics and Biosensing Open Innovation Laboratory, National Institute of Advanced Industrial Science and Technology, Osaka 5650871, Japan; Graduate School of Frontier Biosciences, Osaka University, Osaka 5650871, Japan;* Present Address: Department of Chemistry, Division of Molecular Materials Science, Graduate School of Science, Osaka City University, 3-3-138, Sugimoto, Sumiyoshi, Osaka 5588585, Japan; orcid.org/0000-0002-5065-3021

Yasunori Nawa − *Advanced Photonics and Biosensing Open Innovation Laboratory, National Institute of Advanced Industrial Science and Technology, Osaka 5650871, Japan; Department of Applied Physics, Graduate School of Engineering, Osaka University, Osaka 5650871, Japan*

Shunsuke Tokumitsu − *Advanced Photonics and Biosensing Open Innovation Laboratory, National Institute of Advanced Industrial Science and Technology, Osaka 5650871, Japan; Department of Applied Physics, Graduate School of Engineering, Osaka University, Osaka 5650871, Japan*

Takahiro Nagano − *Advanced Photonics and Biosensing Open Innovation Laboratory, National Institute of Advanced Industrial Science and Technology, Osaka 5650871, Japan; Department of Applied Physics, Graduate School of Engineering, Osaka University, Osaka 5650871, Japan*

Makoto Kawarai − *Advanced Photonics and Biosensing Open Innovation Laboratory, National Institute of Advanced Industrial Science and Technology, Osaka 5650871, Japan; Department of Applied Physics, Graduate School of Engineering, Osaka University, Osaka 5650871, Japan*

Hirokazu Tanaka − *Advanced Photonics and Biosensing Open Innovation Laboratory, National Institute of Advanced Industrial Science and Technology, Osaka 5650871, Japan; Department of Applied Physics, Graduate School of Engineering, Osaka University, Osaka 5650871, Japan*

Tatsuki Hamamoto − *Advanced Photonics and Biosensing Open Innovation Laboratory, National Institute of Advanced Industrial Science and Technology, Osaka 5650871, Japan; Graduate School of Frontier Biosciences, Osaka University, Osaka 5650871, Japan*

Wataru Minoshima − *Advanced Photonics and Biosensing Open Innovation Laboratory, National Institute of Advanced Industrial Science and Technology, Osaka 5650871, Japan; Department of Chemistry, Division of Molecular Materials Science, Graduate School of Science, Osaka City University, Osaka 5588585, Japan*

Tomomi Tani − *Biomedical Research Institute, National Institute of Advanced Industrial Science and Technology, Osaka 5650871, Japan*

Satoshi Fujita − *Advanced Photonics and Biosensing Open Innovation Laboratory, National Institute of Advanced Industrial Science and Technology, Osaka 5650871, Japan; Department of Applied Physics, Graduate School of Engineering, Osaka University, Osaka 5650871, Japan*

Hidekazu Ishitobi − *Advanced Photonics and Biosensing Open Innovation Laboratory, National Institute of Advanced Industrial Science and Technology, Osaka 5650871, Japan; Graduate School of Frontier Biosciences, Osaka University, Osaka 5650871, Japan; Department of Applied Physics, Graduate School of Engineering, Osaka University, Osaka 5650871, Japan;* orcid.org/0000-0002-1145-6850

Complete contact information is available at: https://pubs.acs.org/10.1021/acsomega.1c07206

Author Contributions

Dr. K.M. conceptualized this study, analyzed the results, prepared the figures, implemented the result discussion, and wrote the paper. Dr. Y.N. constructed a program for data analysis and provided a discussion of the data. S.T., T.N., M.K., H.T., and T.H. carried out the experiments, analyzed the data, and implemented the result discussion. Dr. S.F. provided a suggestion about the synthesis method of artificial liposomes. Dr. C.H., Dr. H.I., and Dr. Y.I. provided a discussion of the experimental results. Dr. W.M. and Dr. T.T. provided the biological interpretation. All contributors discussed about the results and corrected the draft.

Funding

This study was supported by the Advanced Photonics and Biosensing Open Innovation Laboratory, National Institute of Advanced Industrial Science and Technology (AIST), and partly supported by JSPS KAKENHI Grant Nos. JP20K15143 (M.W.), JP17H01820 (C.H.), and JP16H06504 (C.H.).

Notes

The authors declare no competing financial interest.

■ ACKNOWLEDGMENTS

The authors thank Dr. Riki Toita for providing suggestions for liposome synthesis. They also thank Dr. Ryugo Tero for a lecture on liposome synthesis and for providing suggestions for all parts of liposome synthesis.

■ REFERENCES

(1) Nicholls, D. G. The glutamatergic nerve terminal. *Eur. J. Biochem* **1993**, *212*, 613−631.

(2) Meldrum, B. S. Glutamate as a Neurotransmitter in the Brain: Review of Physiology and Pathology. *J. Nutr.* **2000**, *130*, 1007S−1015S.

(3) Cavelier, P.; Attwell, D. Neurotransmitter depletion by bafilomycin is promoted by vesicle turnover. *Neurosci Lett.* **2007**, *412*, 95−100.

(4) Hori, T.; Takahashi, T. Kinetics of Synaptic Vesicle Refilling with Neurotransmitter Glutamate. *Neuron* **2012**, *76*, 511−517.

(5) Riveros, N.; Fiedler, J.; Lagos, N.; Muñoz, C.; Orrego, F. Glutamate in Rat Brain Cortex Synaptic Vesicles: Influence of the Vesicle Isolation Procedure. *Brain Res.* **1986**, *386*, 405−408.

(6) Burger, P. M.; Mehl, E.; Cameron, P. L.; Maycox, P. R.; Baumert, M.; Lottspeich, F.; De Camilli, P.; Jahn, R. Synaptic Vesicles Immunoisolated from Rat Cerebral Cortex Contain High Levels of Glutamate. *Neuron* **1989**, *3*, 715−720.

(7) Wang, Y.; Fathali, H.; Mishra, D.; Olsson, T.; Keighron, J. D.; Skibicka, K. P.; Cans, A. Counting the Number of Glutamate Molecules in Single Synaptic Vesicles. *J. Am. Chem. Soc.* **2019**, *141*, 17507−17511.

(8) Takamori, S.; Holt, M.; Stenius, K.; Lemke, E. A.; Grønborg, M.; Riedel, D.; Urlaub, H.; Schenck, S.; Brügger, B.; Ringler, P.; Müller, S. A.; Rammner, B.; Gräter, F.; Hub, J. S.; De Groot, B. L.; Mieskes, G.; Moriyama, Y.; Klingauf, J.; Grubmüller, H.; Heuser, J.; Wieland, F.; Jahn, R. Molecular Anatomy of a Trafficking Organelle. *Cell* **2006**, *127*, 831−846.

(9) Zampighi, G. A.; Serrano, R.; Vergara, L. V. A Novel Synaptic Vesicle Fusion Path in the Rat Cerebral Cortex: The "Saddle" Point Hypothesis. *PLoS One* **2014**, *9*, No. e100710.

(10) Budzinski, K. L.; Allen, R. W.; Fujimoto, B. S.; Kensel-Hammes, P.; Belnap, D. M.; Bajjalieh, S. M.; Chiu, D. T. Large Structural Change in Isolated Synaptic Vesicles upon Loading with Neurotransmitter. *Biophys. J.* **2009**, *97*, 2577−2584.
(11) Palonpon, A. F.; Ando, J.; Yamakoshi, H.; Dodo, K.; Sodeoka, M.; Kawata, S.; Fujita, K. Raman and SERS microscopy for molecular imaging of live cells. *Nat. Protoc.* **2013**, *8*, 677−692.
(12) Hu, F. H.; Shi, L. X.; Min, W. Biological imaging of chemical bonds by stimulated Raman scattering microscopy. *Nat. Methods* **2019**, *16*, 830−842.
(13) Ajito, K.; Torimitsu, K. Laser trapping and Raman spectroscopy of single cellular organelles in the nanometer range. *Lab Chip* **2002**, *2*, 11−14.
(14) Ajito, K.; Han, C.; Torimitsu, K. Detection of Glutamate in Optically Trapped Single Nerve Terminals by Raman Spectroscopy. *Anal. Chem.* **2004**, *76*, 2506−2510.
(15) Cherney, D. P.; Conboy, J. C.; Harris, J. M. Optical-Trapping Raman Microscopy Detection of Single Unilamellar Lipid Vesicles. *Anal. Chem.* **2003**, *75*, 6621−6628.
(16) Bendix, P. M.; Oddershede, L. B. Expanding the Optical Trapping Range of Lipid Vesicles to the Nanoscale. *Nano Lett.* **2011**, *11*, 5431−5437.
(17) Enciso-Martinez, A.; van der Pol, E.; Lenferink, ATM.; Terstappen, L. W. M. M.; Leeuwen, T. G. V.; Otto, C. Synchronized Rayleigh and Raman scattering for the characterization of single optically trapped extracellular vesicles. *Nanomedicine* **2020**, *24*, No. 102109.
(18) Penders, J.; Pence, I. J.; Horgan, C. C.; Bergholt, M. S.; Wood, C. S.; Najer, A.; Kauscher, U.; Nagelkerke, A.; Stevens, M. M. Single Particle Automated Raman Trapping Analysis. *Nat. Commun.* **2018**, *9*, No. 4256.
(19) Sanderson, J. M.; Ward, A. D. Analysis of liposomal membrane composition using Raman tweezers. *Chem. Commun.* **2004**, 1120−1121.
(20) Cherney, D. P.; Harris, J. M. Confocal Raman Microscopy of Optical-Trapped Particles in Liquids. *Annu. Rev. Anal. Chem.* **2010**, *3*, 277−297.
(21) Hosokawa, C.; Kudoh, S.N.; Kiyohara, A.; Taguchi, T. Optical trapping of synaptic vesicles in neurons. *Appl. Phys. Lett.* **2011**, *98*, No. 163705.
(22) Yang, J.; Zhang, R. N.; Liu, D. J.; Zhou, X.; Shoji, T.; Tsuboi, Y.; Yan, H. Laser trapping/confocal Raman spectroscopic characterization of PLGA-PEG nanoparticles. *Soft Matter* **2018**, *14*, 8090−8094.
(23) Shoji, T.; Nohara, R.; Kitamura, N.; Tsuboi, Y. A method for an approximate determination of a polymer-rich-domain concentration in phase-separated poly(N-isopropylacrylamide) aqueous solution by means of confocal Raman microspectroscopy combined with optical tweezers. *Anal. Chim. Acta* **2015**, *854*, 118−121.
(24) Urquidi, O.; Brazard, J.; LeMessurier, N.; Simine, L.; Adachi, T. *Optical Spectroscopy of Crystal Nucleation One Nucleus at a Time*; Cambridge Open Engage: Cambridge, 2021.
(25) Torchilin, V. P. Recent advances with liposomes as pharmaceutical carriers. *Nat. Rev. Drug Discovery* **2005**, *4*, 145−160.
(26) Akbarzadeh, A.; Rezaei-Sadabady, R.; Davaran, S.; Joo, S. W.; Zarghami, N.; Hanifehpour, Y.; Samiei, M.; Kouhi, M.; Nejati-Koshki, K. Liposome: classification, preparation, and applications. *Nanoscale Res. Lett.* **2013**, *8*, No. 102.
(27) Regan, D.; Williams, J.; Borri, P.; Langbein, W. Lipid Bilayer Thickness Measured by Quantitative DIC Reveals Phase Transitions and Effects of Substrate Hydrophilicity. *Langmuir* **2019**, *35*, 13805−13814.
(28) Xi, W.; Haes, A. J. Elucidation of HEPES Affinity to and Structure on Gold Nanostars. *J. Am. Chem. Soc.* **2019**, *141*, 4034−4042.
(29) Zhu, G.; Zhu, X.; Fan, Q.; Wan, X. Raman spectra of amino acids and their aqueous solutions. *Spectrochim. Acta, Part A* **2011**, *78*, 1187−1195.
(30) Peica, N.; Lehene, C.; Leopold, N.; Schlücker, S.; Kiefer, W. Monosodium glutamate in its anhydrous and monohydrate form: Differentiation by Raman spectroscopies and density functional calculations. *Spectrochim. Acta, Part A* **2007**, *66*, 604−615.
(31) Czamara, K.; Majzner, K.; Pacia, M. Z.; Kochan, K.; Kaczor, A.; Baranska, M. Raman spectroscopy of lipids: a review. *J. Raman Spectrosc.* **2015**, *46*, 4−20.
(32) Mashaghi, A.; Swann, M.; Popplewell, J.; Textor, M.; Reimhult, E. Optical Anisotropy of Supported Lipid Structures Probed by Waveguide Spectroscopy and Its Application to Study of Supported Lipid Bilayer Formation Kinetics. *Anal. Chem.* **2008**, *80*, 3666−3676.
(33) Yamanaka, M.; Saito, K.; Smith, N. I.; Arai, Y.; Uegaki, K.; Yonemaru, Y.; Mochizuki, K.; Kawata, S.; Nagai, T.; Fujita, K. Visible-wavelength two-photon excitation microscopy for fluorescent protein imaging. *J. Biomed. Opt.* **2015**, *20*, No. 101202.
(34) Hosokawa, C.; Yoshikawa, H.; Masuhara, H. Cluster formation of nanoparticles in an optical trap studied by fluorescence correlation spectroscopy. *Phys. Rev. E* **2005**, *72*, No. 021408.
(35) Masui, K.; Shoji, S.; Asaba, K.; Rodgers, T. C.; Jin, F.; Duan, X. M.; Kawata, S. Laser fabrication of Au nanorod aggregates microstructures assisted by two-photon polymerization. *Opt. Express* **2011**, *19*, 22786−22796.
(36) Laouini, A.; Jaafar-Maalej, C.; Limayem-Blouza, I.; Sfar, S.; Charcosset, C.; Fessi, H. Preparation characterization and applications of liposomes state of the art. *J. Colloid Interface Sci.* **2012**, *1*, 147−168.
(37) Schweizer, F. E.; Ryan, T. A. The synaptic vesicle: cycle of exocytosis and endocytosis. *Curr. Opin. Neurol.* **2006**, *16*, 298−304.
(38) Ikeda, K.; Bekkers, J. M. Counting the number of releasable synaptic vesicles in a presynaptic terminal. *Proc. Natl. Acad. Sci. U.S.A.* **2009**, *106*, 2945−2950.
(39) Atluri, P. P.; Ryan, T. A.; et al. The Kinetics of Synaptic Vesicle Reacidification at Hippocampal Nerve Terminals. *J. Neurosci.* **2006**, *26*, 2313−2320.
(40) Tero, R. Substrate Effects on the Formation Process, Structure and Physicochemical Properties of Supported Lipid Bilayers. *Materials* **2012**, *5*, 2658−2680.
(41) Jenkins, A. L.; Larsen, R. A.; Williams, T. B. Characterization of amino acids using Raman spectroscopy. *Spectrochim. Acta, Part A* **2005**, *61*, 1585−1594.
(42) Jamieson, L. E.; Li, A.; Faulds, K.; Graham, D. Ratiometric analysis using Raman spectroscopy as a powerful predictor of structural properties of fatty acids. *R. Soc. Open Sci.* **2018**, *5*, No. 181483.
(43) Murakami, K.; Kajimoto, S.; Shibata, D.; Kuroi, K.; Fujii, F.; Nakabayashi, T. Observation of liquid−liquid phase separation of ataxin-3 and quantitative evaluation of its concentration in a single droplet using Raman microscopy. *Chem. Sci.* **2021**, *12*, 7411−7418.

https://doi.org/10.1021/acsomega.1c07206
ACS Omega 2022, 7, 9701−9709